

First T3B Results - Initial Study of the Time of First Hit in a Scintillator-Tungsten HCAL

The CALICE Collaboration*

This note contains preliminary CALICE results, and is for the use of members of the CALICE Collaboration and others to whom permission has been given.

ABSTRACT: We present the first study of the time structure of hadronic showers in the CALICE scintillator-tungsten sampling calorimeter by measuring the time of the first hit in a special timing layer, the T3B setup, about $4 \lambda_l$ deep in the calorimeter. This preliminary study, performed on incompletely calibrated data, is compared to Geant4 simulations and shows very good agreement between data and simulations for a model that includes high precision neutron tracking, while large discrepancies are observed for simulations without this component.

*Corresponding authors: Frank Simon (fsimon@mpp.mpg.de), Christian Soldner (soldner@mpp.mpg.de), Lars Weuste (weuste@mpp.mpg.de)

Contents

1. Introduction	1
2. The T3B Setup	2
3. Data Analysis	3
4. First Simulation Studies	6
5. Results	8
6. Summary	9

1 Introduction

For detector systems at CLIC [1], a hadronic calorimeter using tungsten absorbers is being considered to achieve a compact detector construction allowing the full containment of highly energetic jets while satisfying the space constraints imposed by the solenoidal magnet of the experiments. The high level of hadronic background from $\gamma\gamma \rightarrow$ hadrons, combined with the bunch to bunch spacing of 0.5 ns, requires aggressive time stamping to limit the impact of this background on physics measurements.

In the hadron calorimeter, the precision of timing is not only given by the detector technology, but also by the time structure of the hadronic cascade itself. This structure is influenced by fast components of essentially instantaneous energy deposits from high-energy charged hadrons and from electromagnetic sub-showers, and by slow components from neutrons and photons from nuclear processes. Apart from the shower physics, the time structure of the calorimeter response is also influenced by the sensitive medium and by the detector electronics. The choice of the sensitive medium strongly affects the sensitivity of the detector to different components of the hadronic cascade, such as highly energetic charged particles, photons and neutrons, which each have a different time evolution. In addition, time constants of the medium itself, such as decay times in scintillators, affect the measurement.

Since the evaluation of the performance of calorimetry at a CLIC detector relies on simulations based on GEANT4, it is crucial to study how well the time structure of the detector response for hadronic showers in a tungsten calorimeter is reproduced by the simulations. To provide first measurements for a calorimeter using plastic scintillators, the Tungsten Timing Test Beam (T3B) setup has been installed in the CALICE scintillator tungsten calorimeter (WHCAL) prototype, which was taking data in a first test beam campaign at the CERN PS in Fall 2010.

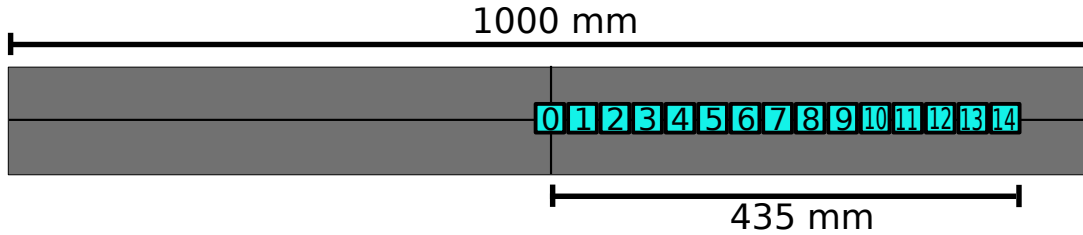


Figure 1. Layout of the T3B scintillator tiles. From the nominal beam axis, the setup extends by 15 mm to one and 435 mm to the other side.

24 2. The T3B Setup

25 The T3B setup consists of fifteen $3 \times 3 \text{ cm}^2$ scintillator tiles with a thickness of 5 mm, directly
 26 read out with 1 mm^2 Hamamatsu MPPC50P SiPMs with four hundred $50 \times 50 \mu\text{m}^2$ pixels. The
 27 scintillator tiles have a “dimple” drilled into the side face at the SiPM coupling position to achieve
 28 a uniform response over the full active area. Variations of the response over the surface area are
 29 smaller than 5% over most of the tile surface [2]. The SiPMs with $50 \times 50 \mu\text{m}^2$ pixels (instead
 30 of $25 \times 25 \mu\text{m}^2$ pixels used for the studies discussed in [2]) have been chosen due to their in-
 31 creased photon detection efficiency in order to provide better sensitivity to small energies, which
 32 is of particular importance for late energy deposits in the hadronic cascade. The T3B scintillator
 33 tiles provide a signal of approximately 27 photo electrons (p.e.) for minimum ionizing particles,
 34 including afterpulses of the photon sensor. The response to muons is discussed in more detail in
 35 Section 3.

36 The photon sensors are read out with 4-channel USB oscilloscopes¹ with 1.25 GS per second,
 37 using long acquisition windows of $2.4 \mu\text{s}$ per event to record the time structure of the energy
 38 deposits in the scintillator in detail. Each SiPM was connected to a preamplifier board (as described
 39 in [2]), which then feeds the signal to the oscilloscope via coaxial cable. The bias voltage for
 40 each channel was adjusted by a resistor divider network, which was powered from one common
 41 high voltage source. The scintillator cells were individually packaged in light-tight tape. The
 42 preamplifier boards with packaged scintillator cells were mounted on a 2 mm thick aluminum plate
 43 and protected by a 1 mm thick aluminum top cover, forming a robust cassette.

44 The T3B scintillator tiles are arranged in one row extending from the center of the calorimeter
 45 layer out to one side of the detector. The first tile is centered on the nominal beam position, thus
 46 the setup extends 15 mm beyond the nominal beam center on one and 435 mm on the other side,
 47 as shown in Figure 1. This permits the measurement of a full radial timing profile of the hadronic
 48 shower at the position of T3B, given sufficient statistics. The limited coverage however only allows
 49 averages over many events to be measured, and is not suitable for the study of the time evolution
 50 on an event by event basis.

51 In the 2010 test beam period, the T3B setup was installed behind the last layer of the CALICE
 52 WHCAL, which consisted of 30 tungsten absorber plates, 1 cm thick, supported by a 1 mm thick
 53 steel plate in addition. Behind each of the 30 absorber layers, one active layer of the CALICE
 54 analog HCAL [3] was installed. After those 30 layers, additional slots without absorber plates

¹PicoTech PicoScope 6403 (<http://www.picotech.com/>)

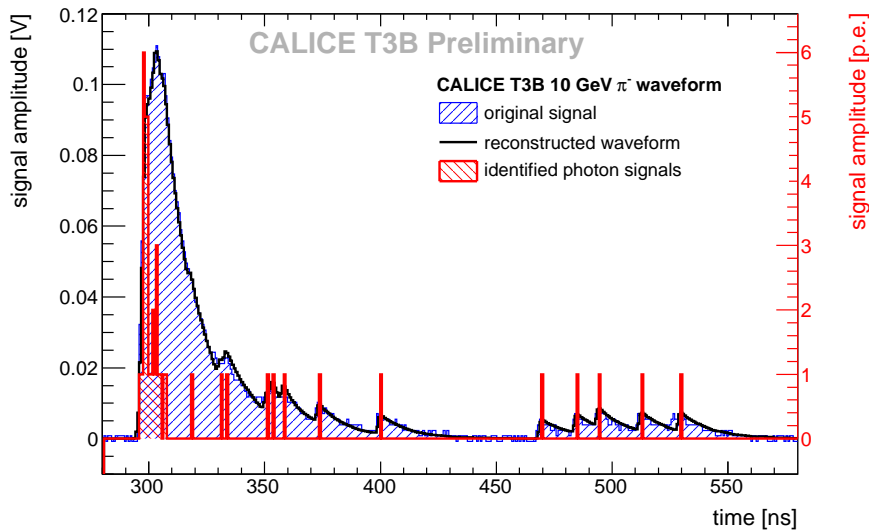


Figure 2. Typical waveform with a high initial signal, decomposed into individual photon signals during the data analysis. Very good agreement of the original waveform and the reconstructed signal from standard single photo-electron distributions is observed.

55 were included in the mechanical structure. The first layer downstream of the calorimeter was used
 56 by a CALICE Micromegas test module [4], while the second downstream layer was occupied by
 57 T3B. The T3B setup was located at a depth of approximately $4 \lambda_I$.

58 During data taking, T3B was triggered by the main CALICE trigger, which will allow a match-
 59 ing of CALICE and T3B events in future analyses. In total, T3B uses four USB oscilloscopes
 60 totaling 16 channels, with the one channel not used for SiPM readout employed to monitor the
 61 signal from the trigger scintillators to allow the rejection of CALICE calibration triggers and the
 62 identification of double particle events. Between spills, T3B was taking dark rate events to allow
 63 a continuous monitoring of the SiPM gain. In future analyses, a correction based on the observed
 64 variations of the gain will be performed, but for the present studies, no corrections were applied.

65 3. Data Analysis

66 For the present note, a data set consisting of approximately 718 000 10 GeV π^- events was ana-
 67 lyzed, using T3B in standalone mode without attempting to correlate the events with CALICE WH-
 68 CAL events to obtain additional information about the showers. The negative beam polarity was
 69 chosen to avoid a contamination with protons. At 10 GeV, the electron contamination of the beam
 70 is negligible, and this highest available energy at the T9 PS beam line provides the largest hadronic
 71 activity, and thus the highest signal statistics in T3B. The muon contamination of the beam, which
 72 was not rejected, was around 10%. The size of the trigger counters limits the influence of muons
 73 to the two central tiles. Data quality cuts reduced the event sample to 645 000 accepted events by
 74 rejecting spills with inconsistent trigger numbers for the four T3B oscilloscopes, most likely linked
 75 to CALICE calibration triggers during the T3B end of spill phase. 58 000 events have an identified
 76 first hit that satisfies the analysis requirements discussed below in one of the T3B cells.

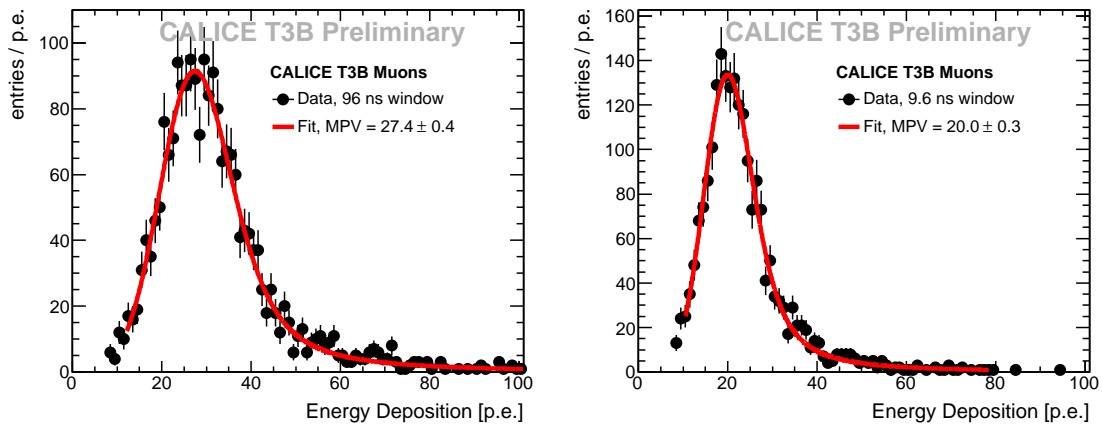


Figure 3. Measured spectrum for muons in the central T3B scintillator tile, reconstructed by identifying the time of individual photon signals in the SiPM, for two different integration time windows: 96 ns from the first identified photon (*left*) and a time window of 9.6 ns (*right*). The distributions were fitted with a Landau function convolved with a Gaussian to extract the most probable value. In both cases, the χ^2 per degree of freedom is around 0.8, indicating a good fit quality.

77 The data were analyzed on a cell by cell level. As a first step, zero suppression based on
 78 pedestals determined on a spill-by-spill basis was applied. Then, a threshold on the total zero-
 79 suppressed integral of the complete waveform equivalent to 0.3 MIP (corresponding to about 8
 80 p.e.) was applied to consider a cell for further analysis in order to reduce the processing time for
 81 the complete data set. Then, the waveform was decomposed into individual photon equivalents to
 82 provide precise information on the arrival time of photons at the light sensor. This was done by
 83 consecutively subtracting single photon signals from local maxima detected in the waveform, until
 84 no maxima above approximately 0.5 p.e. remained. The single photon signals were obtained from
 85 noise events taken between spills and are determined for each tile separately. This results in an im-
 86 plicit gain calibration, since possible cell-to-cell gain differences lead to corresponding differences
 87 in the average single photon signals used in the analysis. The resulting number of photons is thus
 88 independent of the SiPM gain. This reference signal was refreshed every 10 spills, typically corre-
 89 sponding to time intervals of less than 5 minutes. This provided continuous automatic corrections
 90 of gain variations due to temperature changes. The temperature was monitored by one temperature
 91 sensor included in the T3B cassette. The temperature range of the data considered here was on the
 92 order of 0.8 °C, resulting in gain variations of approximately 3%.

93 Figure 2 shows one example of a waveform decomposed using this reconstruction technique.
 94 To check the quality of this analysis, a waveform based on the identified photon signals was built
 95 up with the reference single photon signals and compared to the original waveform. The very
 96 good agreement between measurement and the reconstructed waveform demonstrates the quality
 97 of reconstruction.

98 Figure 3 shows the distribution of the energy reconstructed with this technique in the cen-
 99 tral tile of T3B for muons obtained in a special data run with an absorber in the beam line. The
 100 deposited energy was determined with two different integration windows, 96 ns from the first iden-
 101 tified photons, shown in Figure 3 *left* and 9.6 ns, shown in Figure 3 *right*. The most probable value

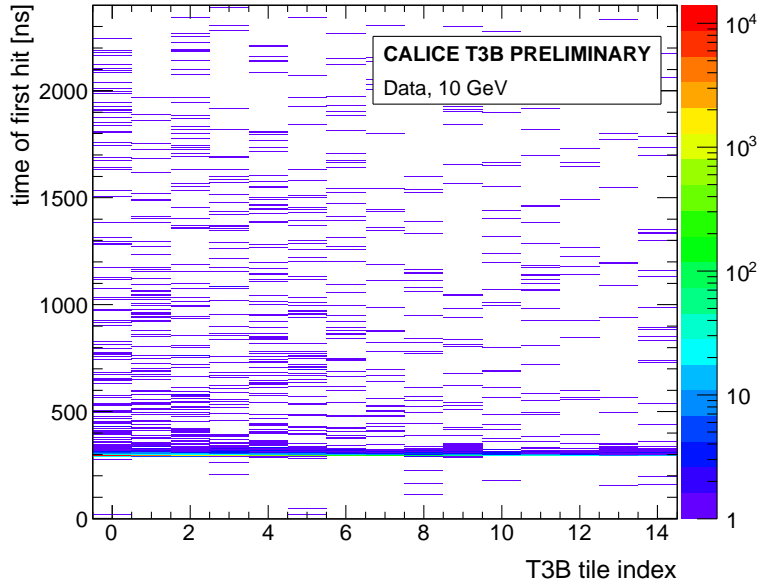


Figure 4. Distribution of the time of first hit for all 15 T3B channels for 10 GeV π^- .

102 of both distributions was extracted by fitting a Landau function convolved with a Gaussian. The
 103 integration time has a considerable effect on the most probable value, which is reduced by almost
 104 30% from 27.4 ± 0.4 p.e. to 20.0 ± 0.3 p.e. for the reduced integration window. Also the width
 105 of the signal is reduced considerably. This is due to the partial exclusion of contributions from
 106 afterpulses of the photon sensor.

107 The final analysis for 10 GeV π^- events was performed on the decomposed waveform, using
 108 the timing of each identified photon. Here, signals were considered where at least 8 p.e. were
 109 detected within 12 time bins (9.6 ns). The narrow time window considered leads to a reduction of
 110 the typical MIP amplitude, since a considerable fraction of the SiPM afterpulses were excluded,
 111 as discussed above. The threshold corresponds to the equivalent of 0.4 MIPs. The time of hit was
 112 then taken from the timing of the second detected photon of that hit. It was observed that using the
 113 first instead of the second photon leads to additional jitter due to single p.e. dark counts before the
 114 starting time of the real hit. At typical dark count rates of a few 100 kHz, the probability for such
 115 events within the integration time window is on the 10^{-3} level. The time of first hit for a T3B cell
 116 is given by the starting time of the first such hit in the waveform.

117 At present, no cell-to-cell calibration is performed, leading to some uncertainty on the overall
 118 MIP scale for each cell. The MIP scale is only determined in the central T3B tiles using muon
 119 data. The result of a fit to muon data in the adjacent tile, which is statistically limited, yields a 5%
 120 lower most probable value, consistent within errors with the fit to the distribution in the central tile.
 121 In general, only small cell-to-cell variations of the light yield are expected for the directly coupled
 122 scintillator tiles used in T3B. For the determination of the time of the first hit in a given cell, this
 123 missing calibration only contributes to higher order corrections from the application of thresholds,
 124 and does not influence the timing measurement itself.

125 Figure 4 shows the distribution of the time of first hit as a function of radial position, given

126 by the T3B cell index, showing the expected cluster of events at early times in coincidence with
127 the timing of the original beam particle, but also considerable late activity in the shower. Further
128 analysis of this distribution, together with simulation studies, are discussed below.

129 **4. First Simulation Studies**

130 Simplified simulations, based on a direct implementation of the WHCAL geometry in Geant4 (ver-
131 sion 4.9.3.p01), were performed to provide first comparisons to the T3B results. In the simulations,
132 the setup was implemented as a 31 layer WHCAL detector, with absorber plates consisting of 10
133 mm tungsten alloy (93% W, 1.8% Cu, 5.2% Ni, density 17.6 g/cm^3) and 1 mm steel. The active
134 modules were simulated according to the CALICE simulation model, with two 2 mm thick steel
135 cover plates, 5 mm thick polystyrene scintillator and additional PCB, cable and fiber and air layers.
136 The T3B setup itself was not explicitly included, but was approximated as the 31st layer of the
137 simulation setup, with the Micromegas detector upstream of T3B taken as an extra absorber layer.
138 While this is not an exact description of the real test beam setup, for the variables studied at present
139 these deviations are assumed not to lead to significant effects on the results.

140 For the simulations, Geant4 was run with a range cut of $50 \mu\text{m}$, and a reduction of the visible
141 energy in the scintillator for slow, heavily ionizing particles was accounted for by using Birks'
142 law [5]. 800 000 events, roughly corresponding to the available real data set, were simulated with
143 the QGSP_BERT and QGSP_BERT_HP physics lists. The latter provides additional high precision
144 neutron tracking, and is expected to give an improved description of the shower evolution in heavy
145 absorbers, while the former is the list mostly used in the simulation of LHC detectors and for linear
146 collider optimization studies. For the events generated for the present study, the high precision
147 neutron tracking increased the required CPU time for event simulation by approximately a factor
148 of five. The beam profile was taken into account by a Gaussian smearing of the primary particle
149 position along the horizontal and vertical axis with a width of 8 mm, motivated by the beam profile
150 measured with the tracking system in the WHCAL test beam.

151 The analysis of the simulation data followed the real data analysis closely. For each of the
152 15 T3B cells, a histogram with the energy deposits as a function of time, with 800 ps resolution,
153 was built for each event. In the histogram filling process, energy deposits were transformed from
154 the energy scale to a calibration scale in units of minimum ionizing particles (MIPs), by taking a
155 conversion factor of $815 \text{ keV} / \text{MIP}$ determined from simulated muons. This transformation allows
156 direct comparison to the real data. A total energy deposit of 0.3 MIP in the full time window of
157 $2.4 \mu\text{s}$ was required for a further analysis of each cell.

158 The Geant4 simulations of the T3B setup do not take into account the time structure of the
159 response of the system to an instantaneous signal. This structure originates from scintillator time
160 constants, photon travel times and SiPM response. This smearing in time was included in the
161 simulations by distributing the number of photons corresponding to the energy deposited in each
162 800 ps time bin according to the time distribution of identified photons in the data for muon signals,
163 which represent instantaneous energy deposits. This distribution was obtained by using the data
164 reconstruction technique described in Section 3 and is shown in Figure 5 *left*. A Landau function
165 with a sigma of 1.3 ns was found to give a good description of the distribution, and was used
166 to provide a parametrization for the simulations. With a more refined analysis, a function which

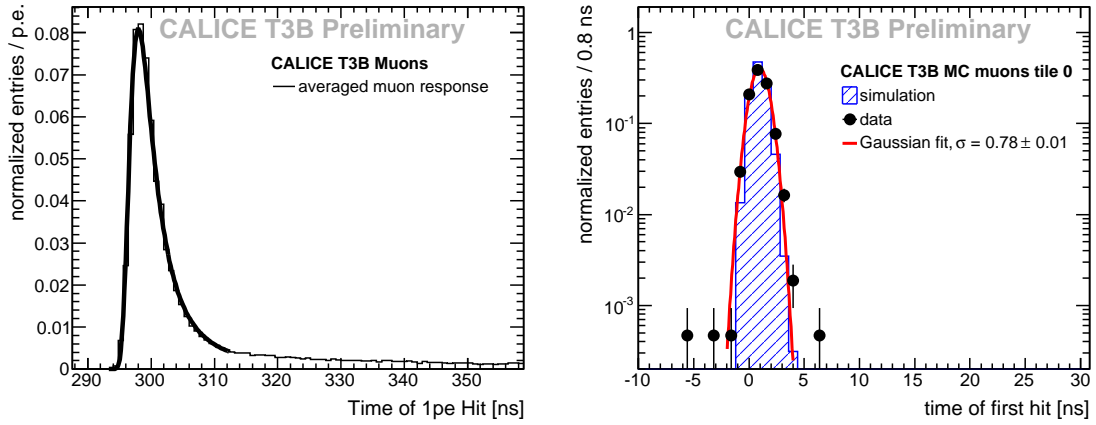


Figure 5. *Right:* Averaged time distribution of the identified photons in muon events. The distribution was fitted with a Landau function, which is used to model the time distribution of individual photons in the simulation. *Left:* Time of first hit for muons in the central T3B tile, compared to simulations. The data points were fitted with a Gaussian to extract the width of the distribution as a measure for the time resolution.

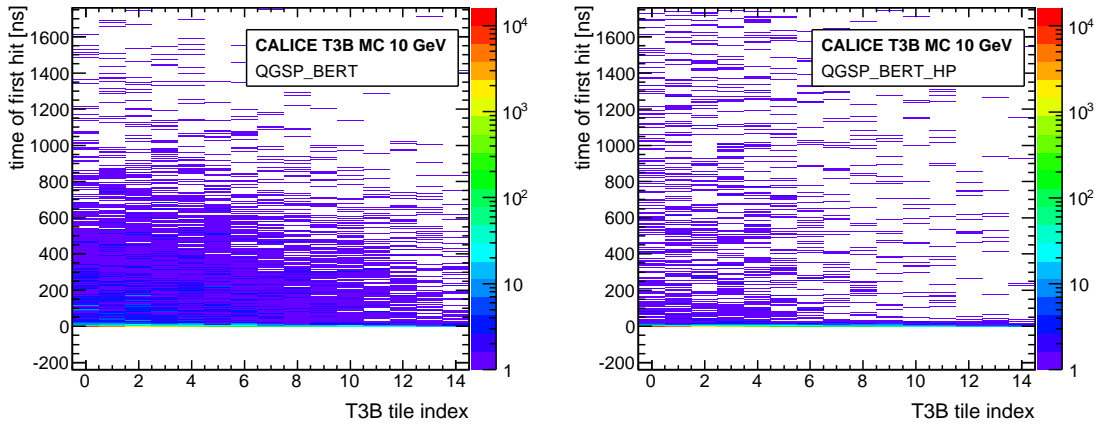


Figure 6. Simulation of the distribution of the time of first hit for all 15 T3B channels for 10 GeV π^- with QGSP_BERT (*left*) and QGSP_BERT_HP (*right*).

167 allows a physical interpretation in terms of scintillator rise and decay times, photon travel times
 168 and photon sensor afterpulsing may be found.

169 Using the parametrization of the signal shape for an instantaneous energy distribution, a simu-
 170 lated photon distribution was built up which was used for further analysis. The time of first hit
 171 was determined from the start of an energy deposit, given by the first bin with an energy above
 172 zero, which contains a minimum of 0.4 MIP within 12 time bins (9.6 ns). Figure 5 *right* shows the
 173 time of first hit determined for muons, compared to simulations with muons using the described
 174 smearing technique. Here, the time of the data distribution is shifted so that the maxima of the two
 175 distributions fall into the same time bin. The good agreement of the simulated distribution and data
 176 validates this parametric inclusion of detector effects on the measured time distributions.

177 The data points were fitted with a Gaussian to extract the width of the distribution as a measure

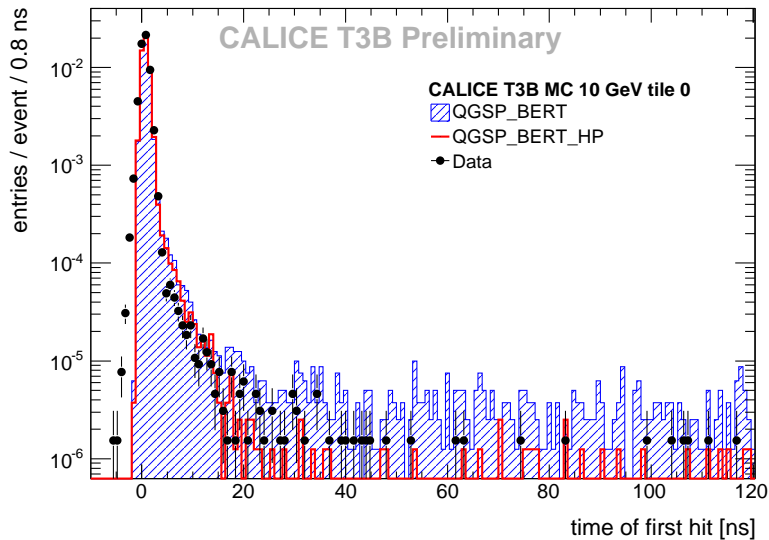


Figure 7. Comparison of the time of first hit distribution in tile 0 simulated for 10 GeV π^- with QGSP_BERT and QGSP_BERT_HP with data.

178 for the time resolution of the T3B system for instantaneous energy deposits. The width of 800 ps
 179 demonstrates that sub-ns resolution, including time jitters of the CALICE trigger system, can be
 180 achieved with the T3B setup for such hits.

181 Figure 6 shows the simulated distribution of the time of first hit over all T3B tiles for the
 182 two considered physics lists, QGSP_BERT and QGSP_BERT_HP for 10 GeV π^- . These figures
 183 illustrate a striking difference in the late shower evolution for the two models. The delayed energy
 184 deposits are considerably reduced in the model including high precision neutron tracking. This
 185 is further demonstrated in Figure 7, which shows the distribution of the time of first hit in the
 186 central tile of T3B which sits close to the beam axis. Here, both physics lists are compared to the
 187 distribution observed in data. The tail of the hit distribution beyond 20 ns is considerably reduced
 188 in QGSP_BERT_HP compared to QGSP_BERT, and is consistent with the observation in data. The
 189 main peak is reasonably well described by both models.

190 5. Results

191 A measure which provides a good indication of the intrinsic time stamping possibilities in the
 192 calorimeter is the time when a cell which contains energy in a given event is first hit. To provide
 193 first robust comparisons between data and simulations, the mean time of first hit for each of the T3B
 194 cells was determined from the distribution of the first hit as discussed in Section 3. The mean was
 195 formed within a time window of 200 ns, starting 10 ns before the maximum of the distribution in
 196 T3B tile 0, and extending to 190 ns after the maximum. This time window covers the time relevant
 197 for calorimetry at CLIC, where the duration for one bunch train is expected to be 156 ns, and is also
 198 comparable to the shaping time of 180 ns used in the front end electronics of the CALICE analog
 199 HCAL modules.

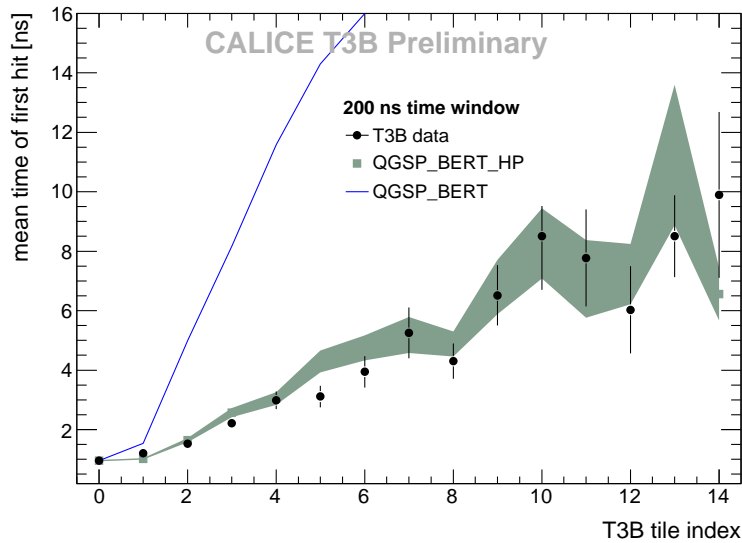


Figure 8. Mean time of first hit for 10 GeV π^- as a function of radial distance from the shower core (a tile index of 10 corresponds to approximately 30 cm). The data are compared with simulations using QGSP_BERT and QGSP_BERT_HP. The error bars and the width of the area in the case of QGSP_BERT_HP simulations show the statistical error, while for QGSP_BERT the errors are omitted for clarity.

200 Figure 8 shows the mean time of first hit as a function of the radial distance from the shower
 201 axis. The beam axis passes through T3B tile 0, so that a tile index of 10 corresponds to a distance
 202 of approximately 30 cm. The measurement is compared to the simulations with the two physics
 203 lists, QGSP_BERT and QGSP_BERT_HP. While QGSP_BERT_HP gives an excellent description
 204 of the data, QGSP_BERT shows very large discrepancies, with significantly overestimated late con-
 205 tributions at larger radii. This demonstrates the importance of the high precision neutron tracking
 206 in Geant4 for a realistic reproduction of the time evolution of hadronic showers in tungsten.

207 6. Summary

208 We have presented first preliminary results of the measurement of one aspect of the time structure
 209 of hadronic showers of 10 GeV π^- in the CALICE scintillator-tungsten hadronic calorimeter at a
 210 depth of approximately $4 \lambda_I$ using the T3B setup. The comparison of the data to simulations per-
 211 formed with a simplified detector model has shown very good agreement for the QGSP_BERT_HP
 212 physics list, while large discrepancies were observed for QGSP_BERT. The use of high precision
 213 neutron tracking reduces the number of late hits considerably, and brings the simulation in agree-
 214 ment with observation.

215 References

- 216 [1] R. W. Assmann, F. Becker, R. Bossart, H. Burkhardt, H.-H. Braun, G. Carron, W. Coosemans,
 217 R. Corsini *et al.*, *A 3-TeV e^+e^- linear collider based on CLIC technology*, CERN-2000-008 (2000).
 218 [2] F. Simon, C. Soldner, *Uniformity Studies of Scintillator Tiles directly coupled to SiPMs for Imaging*
 219 *Calorimetry*, Nucl. Instrum. Meth. **A620**, 196-201 (2010).

- 220 [3] C. Adloff, Y. Karyotakis, J. Repond *et al.*, *Construction and Commissioning of the CALICE Analog*
221 *Hadron Calorimeter Prototype*, JINST **5**, P05004 (2010).
- 222 [4] C. Adloff, D. Attie, J. Blaha, S. Cap, M. Chefdeville, P. Colas, A. Dalmaz, C. Drancourt *et al.*,
223 *MICROMEGAS chambers for hadronic calorimetry at a future linear collider*, JINST **4**, P11023
224 (2009).
- 225 [5] J.B. Birks, *Theory and Practice of Scintillation Counting*, Pergamon Press (1964).